Reprinted from Nature, Vol. 313, No. 6002, pp. 467-470, 7 February 1985
© *Macmillan Journals Ltd., 1985*

Dirty snow after nuclear war

Stephen G. Warren* & Warren J. Wiscombe†

* Department of Atmospheric Sciences, AK-40, University of Washington, Seattle, Washington 98195, USA
† NASA-Goddard Space Flight Center, Greenbelt, Maryland 20771, USA

The notion that smoke from fires started by nuclear explosions could alter the Earth's climate[1] is supported by quantitative models of climate[2–5,27] showing that severe cooling may be expected at continental surfaces in the first few months following a full-scale nuclear war, because of the reduced transmission of sunlight through the atmospheric smoke. Whether or not these model results are correct, we show here that the smoke could continue to cause significant climatic disruption even after it has fallen from the atmosphere, by lowering the reflectivity of snow and sea-ice surfaces, with possible effects on climate in northern latitudes caused by enhanced absorption of sunlight. Indeed, on Arctic sea ice and on the ablation area of the Greenland ice sheet, the reduced reflectivity could persist for several years.

The fraction of light reflected by pure snow is >90% at visible wavelengths, but much lower in the near-infrared. The spectral measurements can essentially be explained by radiative-transfer modelling[6]. As convective and latent-heat transfers over snowpacks are, typically, smaller than the radiative fluxes[7], the energy budget of the snowpack is strongly influenced by the spectrally-averaged albedo

$$\bar{a} = \frac{\int_0^\infty a(\lambda) S(\lambda)\, d\lambda}{\int_0^\infty S(\lambda)\, d\lambda} \qquad (1)$$

where $a(\lambda)$ is the snow albedo (ratio of upward to downward radiation flux) at wavelength λ and $S(\lambda)$ is the spectral distribution of solar energy flux incident on the surface ($W\,m^{-2}\,\mu m^{-1}$). Pure snow reflects 70–85% of the solar energy incident on it, depending primarily on the snow grain size which normally grows as the snow ages[8]; $\bar{a}$ is 80–85% for new snow of grain radius r in the range 50–100 μm and $\bar{a} \simeq 70\%$ for old melting snow ($r \simeq 1$ mm). The albedo is also influenced by solar zenith angle and by cloud cover.

Small amounts of absorptive impurities in snow can reduce the albedo dramatically in spectral regions where it is high (visible wavelengths). We previously computed[9] the radiative effects of graphitic carbon, 'soot' (mass fraction $\leqslant 10^{-7}$) distributed uniformly through a snowpack, and subsequent experiments, measuring both albedo and soot content[10], agreed within the experimental uncertainty (a factor of ~2 in soot content) with predictions of our radiation model[11].

For the present purpose, the earlier results (Fig. 7 and footnote 3 of ref. 9) must be extended to larger amounts of soot and also be averaged over wave-length. The solar spectrum at the Earth's surface, $S(\lambda)$, is obtained using Wiscombe's atmospheric radiation model[12] for the subarctic-summer standard atmosphere[13]. Figure 1 shows the dependence of snow albedo on soot content, for two values of snow grain size. A given amount of soot causes a greater reduction in albedo in old snow than in new snow because the radiation penetrates deeper on average in old coarse-grained snow and therefore encounters more absorbing material before being scattered back out of the snowpack.

Results are also shown of calculations using the optical properties of the 'smoke' for the baseline nuclear war scenario of the US National Academy of Sciences (NAS)[14]. As this smoke contains 20% soot and 80% transparent oily compounds, it is less absorptive than pure soot, but the effects of a given amount of 'smoke' on snow albedo closely match those calculated for pure soot of the amount present in the smoke. Thus, in Fig. 1, by shifting the top scale (for smoke) by a factor of ~5 relative to the bottom scale (for soot), we were able to superimpose the results for 'smoke' on those for 'soot', except in very polluted snow (dashed curves).

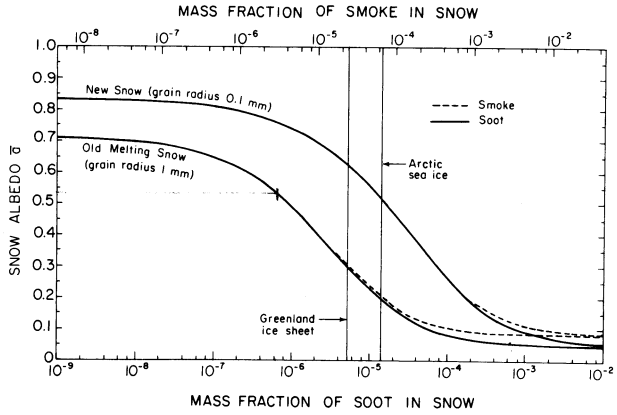

Fig. 1 Spectrally-averaged snow albedo as a function of soot (bottom scale) or smoke (top scale) content, for two different snow grain sizes. (The grain size is the radius of an optically-'equivalent' sphere and is related to the volume/surface ratio of nonspherical snow grains[11].) The spectral complex refractive index of ice is obtained from ref. 24. 'Soot' is assumed to have complex refractive index $1.8 - 0.5i$, independent of wavelength, and density $1.0\,g\,cm^{-3}$ (footnote 3 of ref. 9) and to be present as uniform spheres of radius 0.1 μm. These values imply a mass absorption coefficient for soot decreasing with wavelength from $11.7\,m^2\,g^{-1}$ at $\lambda = 300$ nm to $4.6\,m^2\,g^{-1}$ at $\lambda = 1{,}000$ nm. 'Smoke' also has density $1.0\,g\,cm^{-3}$; its refractive index, $1.55 - 0.1i$, was specified by NAS[14] for visible wavelengths, but is also used here for the near-infrared. This assumption is not crucial, because the major reduction of albedo is at visible wavelengths; pure snow already has low albedo in the near-infrared because of the greater absorptivity of ice there. The smoke has log-normal size distribution with number-mode radius $r_m = 0.1$ μm and log-normal width $\gamma = 2.0$ (Table 5.7 of ref. 14). This distribution has effective radius[25] $r_{eff} = 0.33$ μm. Doubling the mode radius to $r_m = 0.2$ μm ($r_{eff} = 0.66$ μm), to simulate possible aggregation of the smoke particles, would have the same effect as reducing the concentration of smoke in snow by a factor of 1.5. Calculation is for an 'external mixture' of soot particles and ice particles; for an internal mixture the curves should be shifted by a factor of ~2 to the left. The incident solar radiation spectrum is assumed to be that for subarctic summer, clear sky, solar zenith angle 53°, at sea level. A given concentration of impurities would reduce albedo somewhat more under a cloudy sky. Vertical lines give concentrations for the scenarios discussed in the text, for smoke distributed through one month's snowfall.

All these calculations are done by modelling soot or smoke in snow as an 'external mixture' (impurity particles separated from ice particles), which may underestimate the true effect of the impurities as a given reduction of albedo can be achieved by about half as much soot, if the soot is instead located inside the ice grains[15,16] ('internal mixture'). (However, the snow albedos, $\bar{a}$, of Chylek *et al.*[15], are too low because, for $S(\lambda)$ in equation (1), these workers used the solar spectrum at the top of the atmosphere instead of at the snow surface; for example, the absorptivity of pure snow with $r = 0.1$ mm should be 0.17 (Fig. 1 here) instead of 0.21 in their Fig. 7.) The most probable situation, in which smoke is scavenged by falling snow crystals, ending up on the surface of the ice grains[17], would probably give results intermediate between those of external and internal mixtures.

We now use Fig. 1 to estimate the reduction of snow albedo following nuclear war for the case of snow covering the sea ice of the Arctic Ocean, the surrounding tundra of the northern continents and the Greenland ice sheet, areas where the absorption of sunlight would be most enhanced because the effect of changing snow albedo is not muted by forest cover. We use the NAS[14] baseline scenario in which 1.8×10^{14} g of smoke is injected into the atmosphere. Because of its proximity to sources of smoke, the Arctic may suffer more pollution than the average for the Northern Hemisphere, but here we simply assume the smoke is uniformly deposited over the Northern Hemisphere,

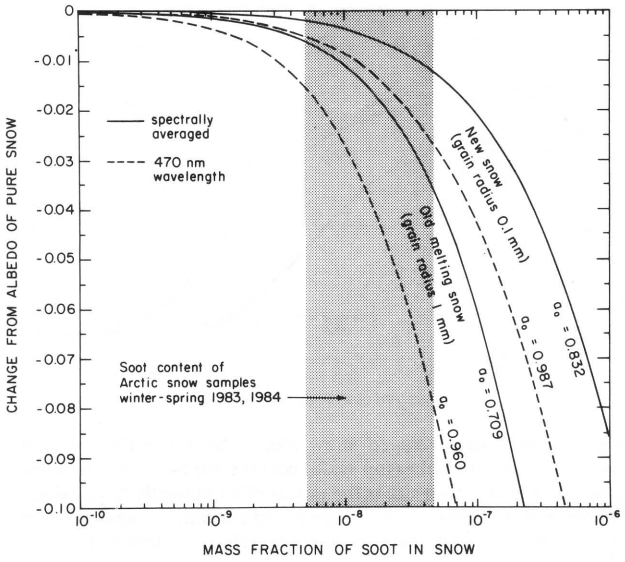

Fig. 2 Computed effects on snow albedo caused by small mass fractions of soot. Soot size distribution and refractive index, snow grain sizes and solar radiation spectrum are the same as used in Fig. 1. The changes from the albedo values of pure snow, a_0, are plotted; the spectrally-averaged changes (solid lines) correspond to the left-most portion of the plots in Fig. 1, on an expanded vertical scale here. The dashed lines are calcuations at the wavelength where snow albedo is most sensitive to soot content ($\lambda = 470$ nm). The reduction in spectrally-averaged albedo is thus approximately half that at visible wavelengths. The shaded region indicates the range of soot concentrations determined[26] in 12 samples of snowfall collected from Arctic Canada, Alaska, Greenland and Svalbard during winter and spring 1983–84. To ensure consistency between soot measurement and albedo calculation, they have been multiplied here by the factor 0.85; previously[26], a mass absorption coefficient $k_{abs} = 8.5\ m^2\ g^{-1}$ for ambient soot at $\lambda = 525$ nm was assumed, whereas the Mie calculation for the soot parameters used here gave $k_{abs} = 10.0\ m^2\ g^{-1}$.

so the total smoke fallout is $0.71\ g\ m^{-2}$. The e-folding decay time for smoke fallout is probably in the range 10–30 days. (For the baseline scenario in Fig. 1 of ref. 2 it is 30 days.) Using an average precipitation of $13\ g\ cm^{-2}\ yr^{-1}$ for the Arctic Ocean[18] and $37\ g\ cm^{-2}\ yr^{-1}$ for Greenland[19], the mass fraction of smoke in the snow would be 6.5×10^{-5} on the Arctic sea ice and 2.2×10^{-5} on Greenland, if distributed through one month's precipitation in each case. These concentrations are indicated by vertical lines in Fig. 1. The values of $\bar{a}$ intersected by these lines indicate that the fraction of solar energy absorbed by snow $(1 - \bar{a})$ on the Arctic Ocean would increase by a factor of 2.8 (new snow)–2.7 (old melting snow) and on Greenland by a factor of 2.2–2.4, respectively. But a net positive effect on the snow energy budget cannot be expected until most of the soot has fallen from the atmosphere so that it no longer blocks the sunlight.

The estimates of smoke concentration in the snow depend, of course, on the snowfall rate and the smoke sedimentation rate and on the total smoke injection into the atmosphere, all of which are highly uncertain. The snowfall rate may be reduced, for example, because of the greater atmospheric stability in the presence of smoke[2]. The vertical lines in Fig. 1, therefore, are only illustrative of the possible magnitude of the effect and are not meant to be quantitative predictions. Other scenarios for different amounts of smoke can be read off Fig. 1, as desired. For example, if the total amount of smoke were the same as we assumed, but fell over a period of two months instead of one (or if it fell quickly, but was distributed through two months snowfall by wind-drifting), the vertical lines should be moved a factor of two to the left, changing the albedo of polluted new snow on Arctic sea ice from 0.52 to 0.60; of old snow from 0.20 to 0.27.

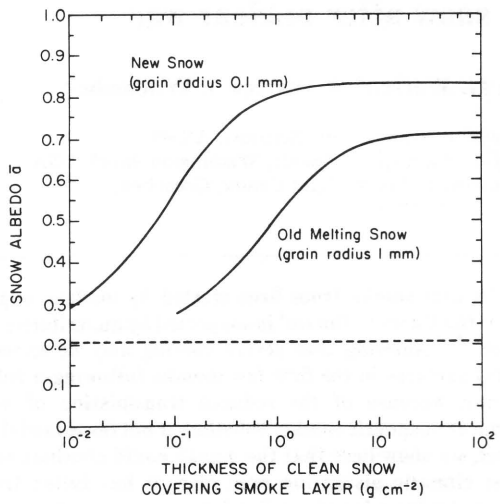

Fig. 3 Spectrally-averaged snow albedo as a function of the thickness of clean snow covering the smoke layer, for two different snow grain sizes. The smoke is assumed to be distributed through a layer of coarse-grained snow, $r = 1$ mm, corresponding to one month's snowfall in the Arctic Ocean, so that it has spectrally-averaged albedo 0.203 when on the surface (intersection of vertical line 'Arctic sea ice' with dashed curve in Fig. 1, shown here as horizontal dashed line). Solar radiation spectrum is the same as for Fig. 1. No calculations are done for snowpack thicknesses less than a monolayer of snow grains.

These hypothetical effects of nuclear war are all much larger than the possible reduction of snow albedo of a few per cent caused by the small concentrations of soot found at present in Arctic snow (Fig. 2).

In the above four cases (intersections of lines in Fig. 1), the polluted layer has sufficient optical thickness for the albedo to be unaffected by the presence of clean snow beneath. However, light penetrates clean snow more deeply than polluted snow. Figure 3 shows how the albedo recovers to high values as the smoke layer is covered by clean snow, assuming for the smoke layer the lowest albedo of the four cases, $\bar{a} = 0.203$. The thickness of clean snow necessary to hide the smoke layer, such that the smoke retains only a 1% effect on $\bar{a}$, is $2\ g\ cm^{-2}$ for new snow and $10\ g\ cm^{-2}$ for old melting snow (corresponding to about 2 and 10 months precipitation in the Arctic, respectively); this means, of course, that as the clean snow ages, its hiding power diminishes.

Although the albedo would rise as clean snowfalls bury the smoke, the polluted layer may be exposed again during a subsequent melt-season and so hasten the disappearance of the snow from the Arctic tundra and sea ice. Experiments are needed to determine whether small smoke particles tend to concentrate at the surface of melting snow, as do micrometre-size dust particles[20].

At high altitude locations on the Greenland ice sheet, the incident solar spectrum $S(\lambda)$ is somewhat different from that used here (compare Fig. 1 caption) but, judging from high-altitude Antarctic calculations[21], the difference in $\bar{a}$ is small enough for these figures still to be used. Unlike the Antarctic ice sheet, where temperatures remain far below freezing throughout the year, in Greenland there is normally some melting in summer over 70% of the ice sheet[19,22]. This melting could be enhanced by smoke fallout, especially in the ablation area of the Greenland ice sheet (~15% of the ice sheet area) where the smoke would be exposed repeatedly in subsequent summers. The effect on the mass budget of Greenland may be estimated from Ambach's model[23].

Persistent consequences would also be expected on multi-year Arctic sea ice. Because the snow now melts completely every summer on Arctic sea ice and because of the direction of sea-ice growth (by freezing at the bottom), the smoke layer would

probably be uncovered repeatedly in subsequent summers to darken the ice.

We thank John Birks, Stephen Schneider and Conway Leovy for encouraging us to do these calculations; Jerry Mahlman for information on smoke lifetime and transport in the atmosphere; Antony Clarke for pre-publication data on soot in Arctic snow; and Walter Ambach, Carl Benson, Arnold Hanson and Starley Thompson for advice. Our research on optical properties of snow and ice is supported by NSF grant ATM-83-15337. The computations were done at the National Center for Atmospheric Research.

Received 11 June; accepted 23 November 1984.

1. Crutzen, P. J. & Birks, J. W. *Ambio* **11,** 114-125 (1982).
2. Turco, R. P., Toon, O. B., Ackerman, T. P., Pollack, J. B. & Sagan, C. *Science* **222,** 1283-1292 (1983).
3. Covey, C., Schneider, S. H. & Thompson, S. L. *Nature* **308,** 21-25 (1984).
4. Thompson, S. L. *et al. Ambio* **13,** 236-243 (1984).
5. Crutzen, P. J., Brühl, C. & Galbally, I. E. *Climatic Change* **6,** 323-364 (1984).
6. Wiscombe, W. J. & Warren, S. G. *J. atmos. Sci.* **37,** 2712-2733 (1980).
7. Paterson, W. S. B. *The Physics of Glaciers* 2nd edn, Ch. 14 (Pergamon, Oxford, 1981).
8. LaChapelle, E. R. *Field Guide to Snow Crystals,* 60-74 (University of Washington Press, 1969).
9. Warren, S. G. & Wiscombe, W. J. *J. atmos. Sci.* **37,** 2734-2745 (1980).
10. Grenfell, T. C., Perovich, D. K. & Ogren, J. A. *Cold Regions Sci. Technol.* **4,** 121-127 (1981).
11. Warren, S. G. *Rev. Geophys. Space Phys.* **20,** 67-89 (1982).
12. Wiscombe, W. J., Welch, R. & Hall, W. *J. atmos. Sci.* **41,** 1336-1355 (1984).
13. McClatchey, R. A., Fenn, R. W., Selby, J. E. A., Volz, F. E. & Garing, J. S. *Optical Properties of the Atmosphere* 3rd edn (AFCRL-72-0497, Air Force Geophysics Laboratory, Hanscom AFB, Massachusetts, 1972).
14. National Academy of Sciences *Report of the Committee on Atmospheric Effects of Nuclear Explosions* (Washington, DC, in the press).
15. Chylek, P., Ramaswamy, V. & Srivastava, V. *J. geophys. Res.* **88,** 10837-10843 (1983).
16. Bohren, C. F. & Hoffman, D. R. *Absorption and Scattering of Light by Small Particles,* 446 (Wiley-Interscience, New York, 1983).
17. Prodi, F. in *Preprints International Conference on Cloud Physics,* 70-75 (American Meteorological Society, Boulder, Colorado, 1976).
18. Vowinckel, E. & Orvig, S. in *Climates of the Polar Regions* (ed. Orvig, S.) 207 (Elsevier, Amsterdam, 1970).
19. Bader, H. *The Greenland Ice Sheet* (CRREL Rep. I-B2, U.S. Army Cold Regions Research and Engineering Laboratory, Hanover, New Hampshire, 1961).
20. Higuchi, K. & Nagoshi, A. in *Isotopes and Impurities in Snow and Ice,* 95-97 (International Association of Hydrological Sciences Publ. No. 118, 1977).
21. Wiscombe, W. J. & Warren, S. G. in *International Radiation Symposium Volume of Extended Abstracts,* 380-382 (Colorado State University, Fort Collins, 1980).
22. Benson, C. S., *Stratigraphic Studies in the Snow and Firn of the Greenland Ice Sheet* (SIPRE Research Rep. 70, U.S. Army Cold Regions Research and Engineering Laboratory, Hanover, New Hampshire, 1962).
23. Ambach, W. *Ann. Glaciol.* **6** (in the press).
24. Warren, S. G. *Appl. Opt.* **23,** 1206-1225 (1984).
25. Hansen, J. E. & Travis, L. D. *Space Sci. Rev.* **16,** 527-610 (1974).
26. Clarke, A. D. & Noone, K. J. *Atmos. Envir.* (in the press).
27. Robock, A. *Nature* **310,** 667-670 (1984).